PAPER • OPEN ACCESS

The effect of elevated dissolved methane concentrations on freshwater phytoplankton: a mesocosm study

To cite this article: Daniel P Gedig and Gregor F Fussmann 2026 *Environ. Res.: Ecology* **5** 035002

View the article online for updates and enhancements.

You may also like

- Methane emissions respond slowly to changes in soil water table depth in contrast to carbon dioxide emissions
Thomas I Marquand, Katy J Faulkner, Bizhou Zhu et al.
- Molecular simulation of methane adsorption characteristics on coal macromolecule
Zhiyuan Yang, Xiaoxiao He, Zhuoyue Meng et al.
- Study to reduce greenhouse gas emissions at waste landfill in Medan City
I Suryati, A Farindah and I Indrawan

This content was downloaded from IP address 216.73.216.56 on 19/11/2026 at 09:02

ENVIRONMENTAL RESEARCH
ECOLOGY

Check for updates

OPEN ACCESS

RECEIVED
17 December 2025

REVISED
8 July 2026

ACCEPTED FOR PUBLICATION
23 July 2026

PUBLISHED
7 August 2026

Original content from this work may be used under the terms of the Creative Commons Attribution 4.0 licence.

Any further distribution of this work must maintain attribution to the author(s) and the title of the work, journal citation and DOI.

PAPER

The effect of elevated dissolved methane concentrations on freshwater phytoplankton: a mesocosm study

Daniel P Gedig[1,2,*] and **Gregor F Fussmann**[1,2]

[1] Department of Biology, McGill University, Montreal, Quebec, Canada
[2] Groupe de recherche interuniversitaire en limnologie (GRIL), Montreal, Quebec, Canada
[*] Author to whom any correspondence should be addressed.

E-mail: daniel.gedig@mail.mcgill.ca and gregor.fussmann@mcgill.ca

Keywords: climate change, eutrophication, greenhouse gases, microbial ecology, phycosphere, oxic

Supplementary material for this article is available online

Abstract

Recent evidence indicates eutrophication will increase freshwater methane (CH_4) production. Aerobic methane-oxidizing bacteria make methane-derived carbon (CH_4-C) available to the aquatic food web, and multiple mechanisms by which phytoplankton may be influenced by the uptake of CH_4-C have recently been proposed. This raises the question of whether lateral interactions within the microbial plankton community might impact freshwater ecosystems as a result of increased CH_4 production. To investigate this, we deployed freshwater mesocosms (750 l polyethylene tanks, $n = 16$) in a temperate lake (Lac Hertel) in southern Quebec, Canada, over a period of thirty days. The mesocosms were aerated with either ambient or CH_4-enriched air and received supplemental nutrients (PO_4^{3-}, NO_3^-) or a control treatment (KCl) to disentangle the influence of increased dissolved CH_4 concentration ($[CH_4]$) and its interaction with nutrient addition. Here we show based on community-level responses that increases in $[CH_4]$ in nutrient-enriched environments may stimulate the growth of certain phytoplankton groups (notably cyanobacteria) and impact ecosystem functioning. Based on our results, we estimated a ∼10% increase in chlorophyll a concentration for implicated phytoplankton groups in a realistic scenario of increased $[CH_4]$. Further, this approach provided unique insights into community-level functioning, such as an estimated 159% increase (33%–577% at 95% confidence) in gross primary production observed in the latter half of the experiment within mesocosms that were both nutrient-enriched and elevated in $[CH_4]$. Although elevating $[CH_4]$ had minimal influence on the net balance of CH_4 (i.e. oxidation versus production), it appeared to stimulate the release of dissolved organic carbon which could have an impact on carbon cycling more generally. Overall, these results suggest that CH_4-C uptake in eutrophic ecosystems may influence phytoplankton community dynamics in the face of global change.

1. Introduction

The key role of inland waters as sources of greenhouse gases to the atmosphere has been established (Cole *et al* 2007, Regnier *et al* 2022), which includes production of the potent greenhouse gas, methane (CH_4) (Saunois *et al* 2020). Aerobic methane-oxidizing bacteria (MOB) can incorporate methane-derived carbon (CH_4-C) and facilitate the transfer of this CH_4-C into the aquatic food web (Jones and Grey 2011, Grey 2016). Increases in freshwater CH_4 production are anticipated due to global changes such as water column deoxygenation (Jane *et al* 2021) and eutrophication (Beaulieu *et al* 2019), which could increase the importance of CH_4-C for the food web as has previously occurred over prehistoric (Saunois *et al* 2020) to industrial (Schilder *et al* 2017) time scales. Microbial interactions underpin these food web dynamics because they are of known importance for MOB (Ho *et al* 2016, Reis *et al* 2024). As a characteristic example, other heterotrophs regulate MOB activity through such interactions (Ho *et al*

© 2026 The Author(s). Published by IOP Publishing Ltd

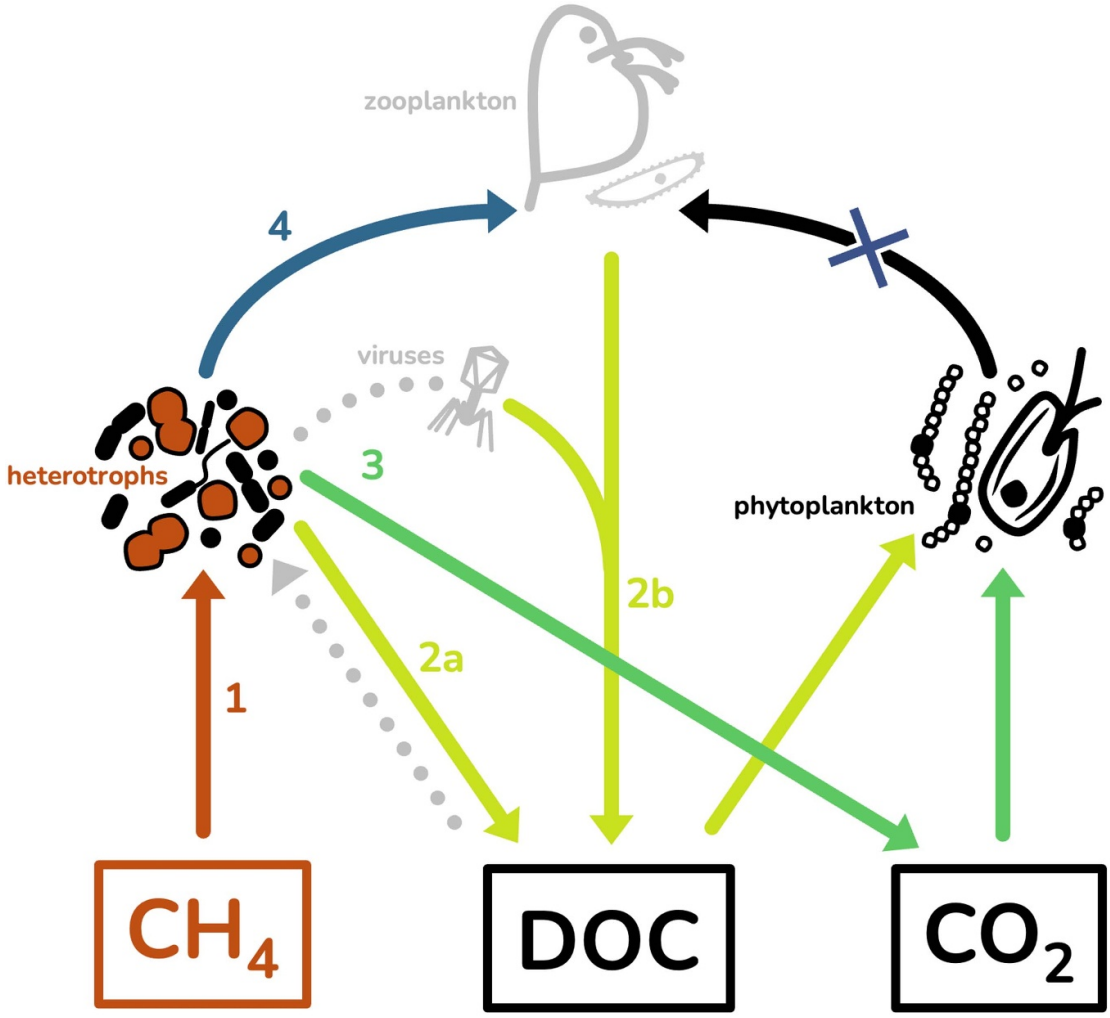


Figure 1. Conceptual figure depicting plausible ecological mechanisms related to the uptake of methane-derived carbon (CH_4-C) in the pelagic food web. Sources of dissolved carbon include methane (CH_4), dissolved organic carbon (DOC), and carbon dioxide (CO_2). (1) Heterotrophs oxidize CH_4. (2) Phytoplankton uptake CH_4-derived compounds from (a) active release or (b) mortality, including lysis and grazing. (3) Phytoplankton use CO_2 produced during oxidation of CH_4 or CH_4-C. (4) Zooplankton graze heterotroph prey sustained by CH_4-C, which may regulate abundances of other microbial prey sources.

2014, 2016) and are therefore implicated in the transfer of CH_4-C to the food web (figure 1, mechanism 1). In this way, microbial dynamics are likely key in how future increases in CH_4-C availability due to increased CH_4 production may impact freshwater ecosystems.

Recently, growing evidence suggests that phytoplankton also interact with MOB and have an important role in CH_4 ecology. This includes niche formation for CH_4-metabolizing microbes (Li *et al* 2021), detection of cyanobacterial genes encoding CH_4 oxidation proteins (Zepernick *et al* 2024), phytoplankton providing oxygen (O_2) to MOB in anoxic environments (Oswald *et al* 2017, Rissanen *et al* 2018), the production of CH_4 during phytoplanktonic photosynthesis (Bizic 2021, Perez-Coronel and Beman 2022), and even the possibility of direct association between phytoplankton and MOB (Cerbin *et al* 2022). As a result of these processes, phytoplankton may uptake CH_4-derived exudates (figure 1, mechanism 2a) or carbon dioxide (CO_2; figure 1, mechanism 3) (Badr *et al* 2022, Cerbin *et al* 2022, Li *et al* 2022). As phytoplankton are generally considered osmotrophic (Glibert 2024a), it is possible that phytoplankton also uptake CH_4-C released during mortality, such as viral lysis or grazing (figure 1, mechanism 2b) (Pernthaler 2017, Glibert 2024b). Capable of both producing CH_4 and incorporating CH_4-C, phytoplankton are likely to be a determining factor in how freshwater ecosystems will respond to increases in CH_4 production.

As oxic zones are generally considered suboptimal for CH_4 oxidation (Thottathil *et al* 2019, Reis *et al* 2022), the transfer of CH_4-C to the pelagic food web has previously been thought to be limited to certain conditions (e.g. stratification, Jones and Grey 2011). However, Crevecoeur *et al* (2019) have stressed that MOB are still present and active in surface waters, and pelagic processes involving CH_4-C indeed

remain important for overall carbon dynamics. For example, zooplankton grazing MOB can reduce CH_4 oxidation rates (Devlin *et al* 2015) and selective grazing of MOB (Ho *et al* 2016 and references therein) may indirectly regulate the abundance of other microbes (figure 1, mechanism 4) (see Kankaala *et al* 2007). Realizing the role of phytoplankton has brought new focus to these pelagic CH_4-C dynamics, yet the way in which individual interactions between microbial functional groups (figure 1) coordinate in natural systems is still largely unknown, a gap in knowledge that we sought to address in our experimental study.

Concretely, our aim was to assess if elevated dissolved CH_4 concentrations ($[CH_4]$) could function as a bottom-up influence and measurably impact microbial dynamics in the pelagic zone. We also examined potential impacts at different levels of nitrogen and phosphorus, considering the role of eutrophication in CH_4 production (Beaulieu *et al* 2019), microbial community composition (Nijman *et al* 2021), and reliance upon alternative trophic strategies (Le Noac'h *et al* 2024), as well as inorganic carbon as a potentially colimiting resource (Katkov *et al* 2020). To this end, our study design assessed the effects of both elevating $[CH_4]$ and enriching inorganic nutrients (N, P) using experimental mesocosms within a temperate lake in southern Quebec, Canada. The primary objective of this study was to investigate how elevated $[CH_4]$ (by itself or in combination with enriched nutrients) affects ecologically relevant response variables, specifically (1) the abundance of major phytoplankton groups and heterotrophic picoplankton and (2) gross primary production (GPP) as a representation of ecosystem functioning. A secondary objective was to assess possible effects of increased $[CH_4]$ on the overall cycling of CH_4 (i.e. net balance of oxidation and production) by incubating water samples and tracking the net change in $[CH_4]$, as well as aquatic carbon cycling as a whole in terms of all carbon species. We hypothesized that elevated $[CH_4]$ would have a stimulatory effect on phytoplankton biomass and GPP, and that higher levels of nitrogen and phosphorus would synergistically enhance this effect by shifting resource constraints on phytoplankton growth that could be alleviated via the mechanisms depicted in figure 1.

2. Methods

2.1. Study area and experimental design

The study area was Lac Hertel within the Gault Nature Reserve located on Mont Saint-Hilaire in southern Quebec, Canada. Lac Hertel is a temperate, dimictic lake with a mean depth of 4.7 m (maximum 8 m) and surface area of 29 ha (Rooney and Kalff 2003). Information on phytoplankton and zooplankton species found previously in Lac Hertel during other studies is provided in the supporting information for reference (tables S1 and S2). We deployed mesocosms in Lac Hertel on a floating dock located 30 m from the shore as in Katkov and Fussmann (2023) and established a factorial experimental design that crossed a $[CH_4]$ increase treatment and a nutrient enrichment treatment. Briefly, cylindrical tanks ($n = 16$, white polyethylene, 750 l capacity) were filled with 487 l of unfiltered lake water using a centrifugal pump on 15 July 2024 (day 0, $t = 0$) such that the depth was approximately 1 m. Tanks were either treated with a control (KCl, to account for potassium addition and changes to charge balance), or with a nutrient enrichment of inorganic phosphorus (H_2KPO_4 and HK_2PO_4 equal in terms of mols P) and nitrogen (KNO_3) in quantities to approximately double the total concentrations of phosphorus and nitrogen in the lake (supporting information figure S1) as in Katkov *et al* (2020). This yielded four mesocosms within each of the four treatment groups. Aeration treatments were introduced to the mesocosms at ∼09:00 local time on day 3, which involved bubbling the tanks on a schedule of 2 min every 4 h. All tanks were fitted with a combination of Torpedo Reinforced Weighted Hose and perforated Bubble Tubing (CanadianPond.ca) that connected to a solenoid gas distribution system via 1.25 cm polyethylene tubing. During the first half of the experiment, each mesocosm was bubbled with either ambient air to reduce the $[CH_4]$, or with a gas mixture elevated in CH_4 (1.2% CH_4, balance air, Linde Canada Inc. Certified Standard) to increase $[CH_4]$ ('CH_4 pulse'). We intended to elevate $[CH_4]$ such that the partial pressure of CH_4 (pCH_4) would be increased by approximately an order of magnitude to 3000 μatm, which was in the range for temperate lakes (22.5°–66.5° N) in data reviewed by Holgerson and Raymond (2016). This target pCH_4 was informed by CH_4 emissions modeled under a future eutrophication scenario (Beaulieu *et al* 2019) that indicated diffusive emissions could rise from 28 Tg CH_4-C y^{-1} (current global mean) to as much as 96 Tg CH_4-C y^{-1} (future upper limit 95% confidence interval), a 240% increase which we use as a benchmark for $[CH_4]$ increase in this study. Beginning on day 15, we initiated a 'post-CH_4' phase by adjusting the aeration treatments so only ambient air was delivered to all tanks. This was done to assess if changes due to elevated $[CH_4]$ would be maintained once $[CH_4]$ was reduced. The mean flow rate of gas to each mesocosm was 5–6 l min^{-1} throughout the experiment.

However, technical issues and fluctuations in the gas distribution network led to variation in, or interruptions of delivered flow. Although this resulted in some differences in pCH_4, we considered the range as a cross-section of possible conditions which was accounted for in statistical analyses described below.

2.2. Sample collection and chemical analyses

Samples were collected from mesocosms and the natural lake for each parameter at a depth of ∼0.2 m. Weekly sampling events started on day 1, with samples for dissolved gases and chemotaxonomic classification (using a Fluoroprobe, described below) of phytoplankton taken weekly afterwards (i.e. five times), and incubation samples for measuring net change in $[CH_4]$, nutrients, and flow cytometric cell counts taken every two weeks afterwards (i.e. three times). As exceptions, an additional sampling event for the natural lake only occurred on day 0, and the samples for chemotaxonomic classification and flow cytometric cell counts attributed to the first event were taken on day 2. Samples from the natural lake were collected from one location near where the mesocosms were deployed for reference and were not subject to statistical analyses. A chart depicting the timing of aeration treatments and sampling events is presented in supporting information figure S2. Samples for dissolved gases ($[CH_4]$ and $[CO_2]$) were collected using the headspace equilibration technique (Koschorreck *et al* 2021). In a 100 ml syringe, 50 ml of sample water was shaken vigorously for 2 min with 50 ml of N_2 (Linde Canada Inc. UHP 99.999%), after which the headspace gas was injected into pre-evacuated vials (12 ml Labco Exetainer) for analysis on a Picarro G2201-i cavity ring-down spectrometer. Solubilities at given water temperature for CH_4 and CO_2 were calculated based on Clever and Young (1987) and Weiss (1974). Unfiltered water samples to measure net change in $[CH_4]$ were collected simultaneously in triplicate in 100 ml borosilicate serum bottles (Wheaton) without headspace and crimp-sealed with a rubber stopper. Bottles were filled by inserting PVC tubing (Nalgene) into the bottom and submerging upside down, using a thumb to partially cover the other end and allowing water to slowly enter without agitation. These samples were incubated in growth chambers and analyzed for $[CH_4]$ using the same technique as *in situ* samples. Incubation conditions and further details are provided in subsection *Methane metabolism incubations*. Samples for chemotaxonomic classification of phytoplankton chlorophyll a (chl a) were collected in polyethylene bottles (Nalgene) by hand dip, i.e. with the mouth of the sampling bottle facing downward when first submerged and rinsing three times with sample water before collection. These samples were kept cool and out of the sunlight for no more than 4 h before analysis on a bench-top Fluoroprobe (bbe Moldaenke, GmbH). This approach uses the fluorescence of chl a and accessory pigments to provide a total chl a concentration, as well as attribute a proportion of the total chl a to a taxonomic group (green algae, Cryptophytes, Heterokonts, or cyanobacteria) as an assessment of community composition (Catherine *et al* 2012). Samples for dissolved organic carbon (DOC) were collected in borosilicate VOA vials (Thermo Scientific) and all other nutrient samples were collected in borosilicate culture tubes (Corning). Samples for total nitrogen and total phosphorus were collected by hand dip. Samples for dissolved nitrogen, dissolved phosphorus, and DOC were filtered (0.45 μm nominal pore size) using a 60 ml syringe, with all tubes triple rinsed with ∼10 ml of filtered sample water before collection. Phosphorus samples were analyzed using potassium persulfate digestion with addition of an acidic ammonium molybdate solution on a Ultrospec 2100pro spectrophotometer following Wetzel and Likens (2000). Nitrogen samples were analyzed using an alkaline persulfate digestion on a continuous flow analyzer (OI Analytical Flow Solution 3100) after Patton and Kryskalla (2003). Carbon samples were analyzed using persulfate oxidation on an OI Analytical Aurora 1030 W TOC Analyzer. Chemical analyses of nutrients and dissolved gases were performed at the GRIL-Université du Québec à Montréal (UQAM) analytical laboratory. Samples for flow cytometry analysis were collected by hand dip and analyzed as described in the *Flow cytometry* subsection.

2.3. GPP estimation

On day 3, miniDOT loggers (Precision Measurement Engineering, Inc.) were deployed in each mesocosm for continuous measurements (every 1 min) of $[O_2]$ (mg l^{-1}) and water temperature (°C) that were used to calculate GPP within the mesocosm tanks. Before deployment, a 24 h $[O_2]$ calibration adjustment of each sensor was performed following manufacturer guidelines in O_2-saturated water between 7.5 and 19.0 °C to correct for drift after factory calibration. Weekly discrete measurements of $[O_2]$ and water temperature (YSI ProSolo, calibrated each day of use) were taken during the experiment (data not shown) and used as an additional validation. The miniDOT sensors were assessed at least once for biofouling during the experiment period. The method principle is derived from Odum (1956) who modeled changes in $[O_2]$ as a function of GPP, ecosystem respiration and diffusion. We used the *LakeMetabolizer* R package (Winslow *et al* 2016) that simultaneously calculated ecosystem respiration and GPP via ordinary least squares regression, with GPP fit as a linear function of photosynthetic photon flux density

(PPFD, μmol m^{-2} s^{-1}). Ecosystem respiration estimates are sensitive to unconstrained physical processes and were uninterpretable in this study due to the aeration treatments, but GPP is considered robust to such influences (e.g. oversaturation, Hall *et al* 2015). Continuously measured meteorological data for ambient air pressure (mbar, every 30 min) and incident solar radiation (W m^{-2}, every 1 min) <1 km south of the experimental site were sourced from the Adaptable Earth Observation System instrument network, financed by the Canadian Foundation for Innovation, the Gouvernement du Québec, McGill University, and UQAM. Incident solar radiation was converted to PPFD using an empirical approximation (Thimijan and Heins 1983) and then smoothed using a 30 min rolling mean. Any gap in the meteorological data ⩾30 min (i.e. due to instrument malfunction) was filled with calculated theoretical clear sky PPFD based on geographic location (Appling *et al* 2018) before smoothing (1756 min total filled, 4.9%). Saturation $[O_2]$ was calculated using ambient pressure and water temperature assuming a salinity of zero following Garcia and Gordon (1992). We used a fixed gas transfer velocity normalized to a Schmidt number 600 of (k_{600}) of 0.6 m d^{-1}, which approximately reflects what was measured using floating chambers in a similar experimental setting (Bogard *et al* 2014) and yielded similar results (supporting information supplementary note 1) when compared to using a conventional approach for variable k_{600} (wind-driven turbulence, Cole and Caraco 1998). This k_{600} value was then scaled to the actual gas transfer velocity for O_2 (k_{gas}) based on water temperature (Raymond *et al* 2012). Data were omitted for 5 min after the start of each aeration event, as well as for 10 min before and after sensor removal during data backups (12 483 min total omitted, 2.2% of all observations). A 30 min rolling mean was then applied to each $[O_2]$ time series to reduce noise, and any omitted data were filled with the last available observation. To prevent rapid changes in $[O_2]$ during aeration events or sensor removal from impacting GPP estimates, the k_{gas} during these data omission periods was calculated such that all changes in $[O_2]$ consistent with the saturation gradient were attributed to diffusion ($k_{gas} \geqslant 0$ m d^{-1}). The GPP estimates were adjusted linearly to a daily mean incident PPFD of 500 μmol m^{-2} s^{-1} and converted into terms of carbon assuming a photosynthetic quotient of 1 mol mol^{-1} (equation (1)),

$$\text{adjusted GPP} = \text{GPP}_{\text{fitted}} \times \frac{500\,\mu\text{mol m}^{-2}\,\text{s}^{-1}}{\bar{x}_{\text{PPFD},t}} \times \frac{\text{mol}_{O_2}}{31.999\ \text{g}} \times \frac{\text{mol}_C}{\text{mol}_{O_2}} \times \frac{12.011\ \text{g}}{\text{mol}_C}. \quad (1)$$

We adjusted in this way to control for variation in PPFD during the experiment while maintaining a value that could be readily compared to other measures of carbon (e.g. [DOC]) as opposed to reporting a radiation-specific value. Due to unique conditions resulting from Tropical Storm Debby, GPP data from one day (9 August 2024) were omitted. Theoretically impossible (i.e. negative) estimates of GPP can be produced when metabolism models are performed without constraints. In order to address this and to minimize error in interpreted values (Staehr *et al* 2010), we pooled GPP estimates by treatment group and calculated the means for two periods: during the CH_4 pulse (before day 15) and post-CH_4 (day 15 and onwards). The R script used for modeling is available via the metaGRIL hosted on borealis, The Canadian Dataverse Repository at https://doi.org/10.5683/SP3/U3U6GY.

2.4. Methane metabolism incubations

To examine the net balance of CH_4 oxidation and CH_4 production in each mesocosm throughout the experiment, we collected unfiltered water samples that were periodically analyzed over the six days following sampling to track the change from the $[CH_4]$ measured *in situ*. This was to assess if the experimental treatments led to disproportionate upregulation of either process. Water samples were transported in transparent containers at ambient temperature until placed in a growth chamber (Conviron CMP6060) in less than 6 h following collection. Samples were kept at a temperature of 26 ± 0.2 °C under a light regime of 18 h light: 6 h dark at 230 μmol m^{-2} s^{-1} (PPFD). A long period of illumination was implemented in the interest of assessing whether substantial net production of CH_4 could occur. Incubations were halted at 16:00 ± 2 h chamber solar time after 1, 3, and 6 d duration (d) for $[CH_4]$ analysis. The possibility of light (Murase and Sugimoto 2005) and O_2 inhibition (Thottathil *et al* 2019) of CH_4 oxidation may have impacted results due to the use of artificial lighting, and the gradual accumulation of O_2 due to relatively lengthy incubation time (e.g. ranged from 24 to 191 h in Thottathil *et al* 2019). However, the intention was to facilitate a relative comparison between treatment groups, and we found these biases due to our methodology would not prevent this. Measurement error as the sample standard deviation of method duplicates ($n = 142$) was found to increase nonlinearly with sample $[CH_4]$ and had a similar range as sample duplicates (supporting information figure S4(a)). Considering this, we determined the coefficient of variation (CV) for method duplicates binned by order of magnitude (supporting information figure S4(b)) and calculated uncertainty (u) as the initial $[CH_4]$ (i.e. *in situ*, C_0) multiplied by the median CV of the corresponding bin. We used normal maximum likelihood estimation to fit parameters of CH_4 production (P, μmol l^{-1} d^{-1}), the first-order rate constant as

is convention for CH_4 oxidation (k, d^{-1}) (Thottathil *et al* 2019), and error of C_0 (ε, μmol l^{-1}) as presented in equation (2). The fitted parameters were discretely iterated for $0 < d < 6$ and the negative log likelihood of the residuals in measured [CH_4] was optimized assuming a distribution of $N(0, u^2)$ (supporting information figure S4(c)),

$$C_{d+1} = C_d e^{-k} + P \tag{2}$$

$$C_0 = C_{0,\text{actual}} + \varepsilon.$$

Optimization was performed with the R function optim() using the L-BFGS-B method (Byrd *et al* 1995) which allows for box constraints. Constraints specified $|\varepsilon| \leqslant u$ and that P and k were non-negative. Initial parameter estimates were conservatively set for P at 0.01 μmol l^{-1} d^{-1} and k at 0.04 d^{-1} based on measured ranges of 0.01–0.52 μmol l^{-1} d^{-1} and 0.04–0.94 d^{-1} in temperate Quebec lakes (Thottathil *et al* 2019, 2022), and for ε at 0 μmol l^{-1}. The net change in [CH_4] was calculated as the difference between measured C_0 (i.e. *in situ* [CH_4]) and fitted C_6, and incubations where ideal convergence was not achieved during fitting were omitted ($n = 2$). Inverse-variance weighting was used in calculating group means and linear models with variance equal to $u^{2.}$ Results were reported as a change in $p$$CH_4$ ($\Delta p$$CH_4$). The R script used for modeling is available via the metaGRIL hosted on borealis, The Canadian Dataverse Repository at https://doi.org/10.5683/SP3/U3U6GY.

2.5. Flow cytometry

In preparation for analysis, 2 ml of whole sample water was transferred into sterile flow cytometry tubes (Falcon 352063). Then, 1 μl of SYTO BC dye (480 nm excitation, 500 nm emission maximum) was added, which is cell-permeant and stains nucleic acids in prokaryotic and eukaryotic cells (Del Giorgio *et al* 1996). The tubes were vortexed for 5 s after staining and then incubated for at least 10 min in the dark at room temperature. Samples were always analyzed the same day as collection which precluded the need for preservative, thus cell morphology was maintained. Samples were analyzed with a five-laser Cytek Aurora spectral flow cytometer on low or medium flow rate (generally $\leqslant$30 μl s^{-1}) at the Flow Cytometry Core Facility (McGill University). The event threshold was set on forward scatter (FSC) and at least 5000 events were recorded for each sample. A polystyrene microsphere standard (6 μm diameter) was used each day of analysis, and all events with an FSC value greater than the median of the standard were omitted to approximately target the picoplankton (0.2–2 μm) fraction (Sieburth *et al* 1978). We acknowledge that cell size and FSC have a complex relationship (Salzman 1999), and that other factors (e.g. refractive index: Model 2018) further complicate assessment of cell size using size references. However, considering the size range most commonly detected with this technique (Del Giorgio *et al* 1996) and in the interest of terminological simplicity, we refer to cells with FSC less than median of the microsphere standard as picoplankton. Events positive (+) for SYTO BC stain (i.e. cells, supporting information figure S5(a)) were identified by 405 nm and 488 nm excitation (ex) and 498–518 nm emission (em). Cells were further categorized by assessing the autofluorescence of chl a (640 nm ex/653–670 nm em) and phycobiliproteins (phyc, 561 nm ex/588–608 nm em) based on the methods outlined in Takahashi (2019) and references therein (supporting information figure S5(b)). Cells that were chl a+ and phyc+ were considered picocyanobacteria, cells that were chl a+ but phyc− were considered picoalgae, and all other cells were considered picoheterotrophs. Although other phytoplankton groups (Cryptophytes, Rhodophytes) can exhibit phyc autofluorescence (Olson *et al* 1989), the size range targeted should exclude most non-cyanobacterial cells that are phyc+. Gates for each day of analysis were set based on the natural lake sample collected the same day (supporting information figure S5). The cell density of each group was calculated by dividing the count in each sample by the total volume analyzed.

2.6. Statistical analyses

Methods of statistical analysis closely follow those of Katkov and Fussmann (2023). For measurements of [CO_2] and of total and group-specific chl a concentrations taken weekly, we fitted a linear model using the lme4 R package (Bates *et al* 2015) with [CH_4] as a continuous variable, nutrient treatment as a dummy variable, and time as a factor with individual mesocosm as a random effect. Estimates of GPP were compared by fitting a similar model, except that [CH_4] treatment and time were instead treated as a dummy variables due to inadequate temporal resolution of [CH_4] measurements and concerns outlined in the *GPP estimation* subsection, respectively. Statistical significance of effects in mixed models was calculated the lmerTest package (Kuznetsova *et al* 2017), and estimated marginal means with 95% confidence intervals were calculated using the emmeans package (Lenth 2024) to represent the effect size of [CH_4] when applicable. We included random effects on the basis

of *a priori* knowledge that data collected at multiple time points from the same mesocosm would be correlated.

For measurements of nutrient concentrations, picoplankton cells counts, and ΔpCH_4 water sample incubations collected biweekly, a linear model was instead fit for each day individually with nutrient and $[CH_4]$ treatments as dummy variables and without random effects. This statistical approach was chosen for these variables as we found there was not enough data to sufficiently characterize interactions of each treatment with time, possibly leading to inaccurate estimation of effect sizes if the model was fit using data from all days. In turn, we opted to code $[CH_4]$ treatments as dummy variables because $[CH_4]$ as a continuous variable would not necessarily reflect treatments that were put in place (i.e. models fit for the last day of the experiment). As a result of these concerns, we do not report effect sizes in the same way as the linear mixed effects models described above.

For all statistical tests, models were iteratively simplified using backwards elimination based on the results of the F-test to remove non-significant terms. Final model results ($\alpha = 0.05$) were reported as the t-statistic of the relevant coefficient with degrees of freedom (df) and corresponding P-values. The normality and homoscedasticity of residuals were assessed by visual inspection of a histogram and a residual plot, respectively. All analyses were performed using R (R Core Team 2024) in RStudio (Posit Team 2023) and data were visualized using the ggplot2 package (Wickham 2016).

3. Results

During the CH_4 pulse (i.e. days 8 and 15), the high $[CH_4]$ mesocosms had a median (minimum—maximum) pCH_4 of 2039 μatm (391–5694 μatm), in contrast to 37.5 μatm (10.7–199 μatm) in the low $[CH_4]$ mesocosms (figure 2(a)). By the end of the experiment (i.e. on day 29), this had decreased to 10.4 μatm (7.6–14.1 μatm) and 5.7 μatm (3.6–7.7 μatm), respectively (figure 2(a)). We found that interaction terms between $[CH_4]$ and time were non-significant ($P > 0.05$) for all variables tested, indicating that any effect of $[CH_4]$ was constant across the experimental period. Statistical results from the F-test used to guide model selection via backwards elimination are presented in supporting information supplementary note 2 for all significant effects reported below. There was no significant effect of $[CH_4]$ on $[CO_2]$ ($t = -1.583$, df = 67.6, $P = 0.12$; figure 2). The median pCO_2 when all treatments were in place (i.e. day 8 and onwards) was 163 μatm (110–228 μatm) in the nutrient-enriched mesocosms and 544 μatm (152–912 μatm) in the mesocosms given the control (figure 2(b)). In the natural lake, the median pCH_4 was 438 μatm (298–629 μatm) and the median pCO_2 was 211 μatm (152–251 μatm) during the experiment (figure 2).

Mesocosms with elevated $[CH_4]$ showed mean net decrease of 50 μatm during the CH_4 pulse (i.e. day 15), a change of −2% relative to the group median pCH_4 that was significantly different ($t = -2.655$, df = 13, $P = 0.02$) (figure 2(c)). Otherwise, mesocosms showed a net increase of 1–4 μatm when all treatments were in effect, which is $\leqslant$1% of the median pCH_4 observed in the natural lake (figure 2(c)). There was no significant main effect of $[CH_4]$ on [DOC] during the CH_4 pulse (i.e. day 15; $t = -0.091$, df = 12, $P = 0.93$), but there was a significant interaction between nutrient enrichment and $[CH_4]$ ($t = 2.370$, df = 12, $P = 0.04$), which indicates elevated $[CH_4]$ significantly increased [DOC] in the nutrient-enriched mesocosms only (figure 2(d)). At the end of the experiment, [DOC] was significantly greater with elevated $[CH_4]$ regardless of nutrient enrichment ($t = 3.779$, df = 13, $P = 0.002$; figure 2(d)).

There was no significant effect of $[CH_4]$ on total chl a ($t = 1.474$, df = 56.3, $P = 0.15$; figure 3(a)). However, there was a significant interaction between nutrient enrichment and $[CH_4]$ for Cryptophyte chl a ($t = 2.301$, df = 66.0, $P = 0.02$) and cyanobacteria chl a ($t = 2.323$, df = 65.8, $P = 0.02$), indicating there was increasing chl a of these groups with greater $[CH_4]$ in the nutrient-enriched tanks only (figure 4). Given a 240% increase scenario from natural lake $[CH_4]$ level (0.604 μmol l^{-1}), Cryptophyte chl a concentration would increase by 0.054 μg l^{-1} (−0.041–0.149 at 95% confidence) or 8.2% (−5.8% to 24.3% at 95% confidence), and cyanobacteria chl a concentration would increase by 0.311 μg l^{-1} (−0.604–1.225 μg l^{-1} at 95% confidence) or 12.3% (−20.4%–60.0% at 95% confidence) based on estimated marginal means (figure 4). At the end of the experiment, picocyanobacteria cell counts were marginally but significantly greater in mesocosms with elevated $[CH_4]$ ($t = 3.468$, df = 13, $P = 0.004$; figure 3(c)), with differences equating to 0.4% (0.06 cells μl^{-1}) and 1.4% (0.2 cells μl^{-1}) of the cyanobacterial cells counts in the natural lake (15.4 cells μl^{-1}) in the control and nutrient-enriched mesocosms, respectively.

There was no significant main effect of $[CH_4]$ treatment on adjusted GPP ($t = 0.068$, df = 22.4, $P = 0.95$), nor interaction between $[CH_4]$ treatment and nutrient enrichment ($t = 0.287$, df = 22.4,

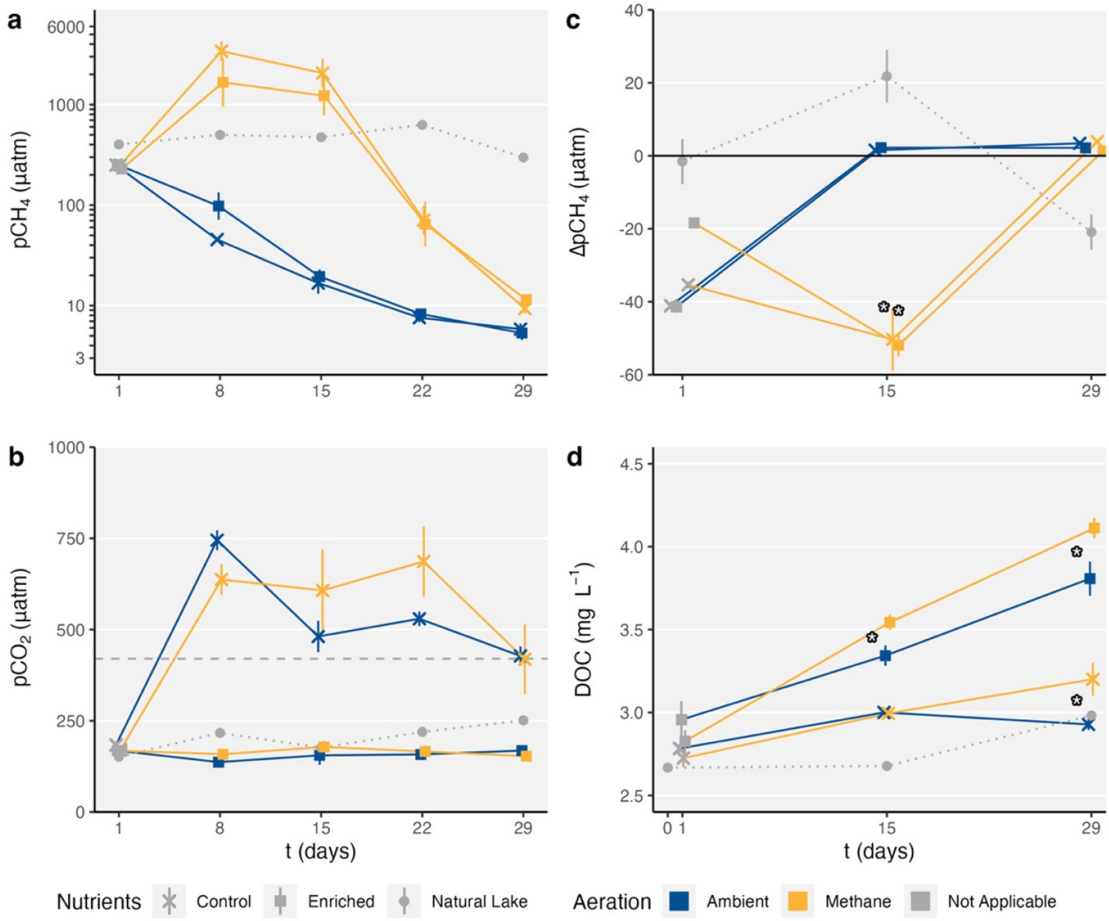


Figure 2. Treatment group means during the experimental period for (a) the partial pressure of methane, (b) the partial pressure of carbon dioxide, (c) weighted groups means of net change in pCH_4 during incubations, (d) dissolved organic carbon concentration. The ΔpCH_4 value was based on the analysis of unfiltered water samples incubated for six days following collection to quantify the net balance of CH_4 oxidation and CH_4 production. Standard error is represented for each mean, and asterisks indicate a significant ($P < 0.05$) effect of applied methane treatment for a given nutrient treatment based on linear models. A line (grey, dashed) indicating approximate pCO_2 saturation (420 μatm) is presented in panel b. Note the logarithmic axis in panel a.

$P = 0.78$; figure 5). However, the three-way interaction term between $[CH_4]$ treatment, nutrient enrichment, and time was significant ($t = 3.052$, df $= 380.0$, $P = 0.002$), which indicates there was a significantly higher mean rate of adjusted GPP in nutrient-enriched mesocosms given the high $[CH_4]$ treatment during the second half of the experiment only (figure 5). We emphasize the conditional and temporally-dependent nature of this effect. This was an increase of 0.438 mg C l^{-1} d^{-1} (0.141–0.735 mg C l^{-1} d^{-1} at 95% confidence) or 159% (33%–577% at 95% confidence) relative to the low $[CH_4]$ treatment based on estimated marginal means (figure 5).

4. Discussion

Despite some variability between mesocosms, an approximately order of magnitude differential in $[CH_4]$ was successfully established between treatment groups during the CH_4 pulse period, or the first half of the experiment. To our knowledge, this is the first time that CH_4 enrichment has been used in an *in situ* mesocosm experiment in the published literature. As expected, the nutrient enrichment treatment manifested greater effects on the phytoplankton community than the elevation of $[CH_4]$ during the experiment. Yet, in line with the focus of our study, we here consider nutrient level only as a variable interacting with the effects of elevated $[CH_4]$. In turn, our hypothesis regarding the interacting effect between nutrient enrichment and elevated $[CH_4]$ was broadly supported. We present a more nuanced interpretation of these results in the following sections.

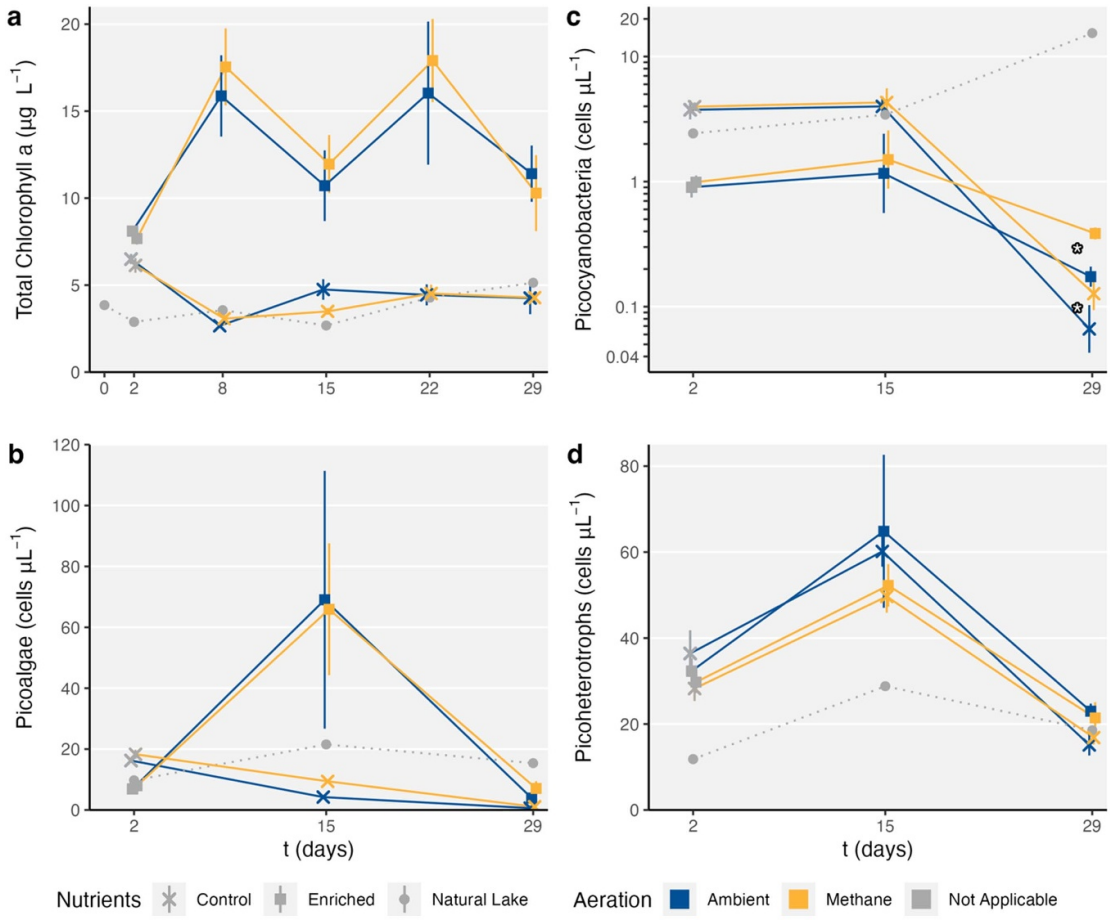


Figure 3. Treatment group means during the experimental period for (a) the total concentration of chlorophyll a, (b) cell counts of picoalgae, (c) picocyanobacteria, (d) picoheterotrophs. Standard error is represented for each mean, and asterisks indicate a significant ($P < 0.05$) effect of applied methane treatment for a given nutrient treatment based on linear models. Note the logarithmic axis in panel c.

4.1. Importance of nutrient level in facilitating effects of methane

Elevation of [CH_4] manifested several changes in the biology and physico-chemical parameters of the simulated ecosystems confined within the experimental mesocosms. However, we observed multiple changes related to elevated [CH_4], particularly those relevant to the phytoplankton community, that only occurred in the nutrient-enriched mesocosms, suggesting that the natural relevance of these interactions would be greater in eutrophic environments. For example, only the nutrient-enriched mesocosms exhibited relatively increased [DOC] during the CH_4 pulse. In contrast, [DOC] in the control mesocosms was only relatively greater at the end of the experiment after the [CH_4] elevation treatment had been terminated. Ultimately, we are unable to ascertain the mechanisms of DOC release based on the data collected here. It is generally recognized that phytoplankton and bacteria exchange organic compounds in aquatic environments (Glibert 2024b), which is a possible direct source of DOC (figure 1, mechanism 2a). Alternatively, loss of substrate after the termination of the [CH_4] elevation treatment may have caused heterotroph mortality (e.g. via viral lysis, Li *et al* 2023) and indirectly led to DOC release (as in figure 1, mechanism 2b).

The increase in chl a observed for cyanobacteria and Cryptophytes specifically in the nutrient-enriched mesocosms might be explained by known characteristics of each phytoplankton group. Cyanobacteria have been widely observed in association with CH_4-metabolizing microbes and involved in CH_4 cycling in eutrophic environments (Li *et al* 2021, Pascault *et al* 2021, Zepernick *et al* 2024). The marginal but significant increase in picocyanobacteria cell counts at the end of the study regardless of nutrient enrichment also supports the notion that the conditions resulting from elevated [CH_4] generally may afford them a small increase in fitness. On the other hand, Cryptophytes are known bacterivores that dominate the mixotroph community in eutrophic environments (Le Noac'h *et al* 2024), although observed rates of bacterial ingestion in Cryptophytes are low and suggest that mixotrophy does not serve as a primary source of carbon, but instead of micronutrients (Tranvik *et al* 1989). Therefore,

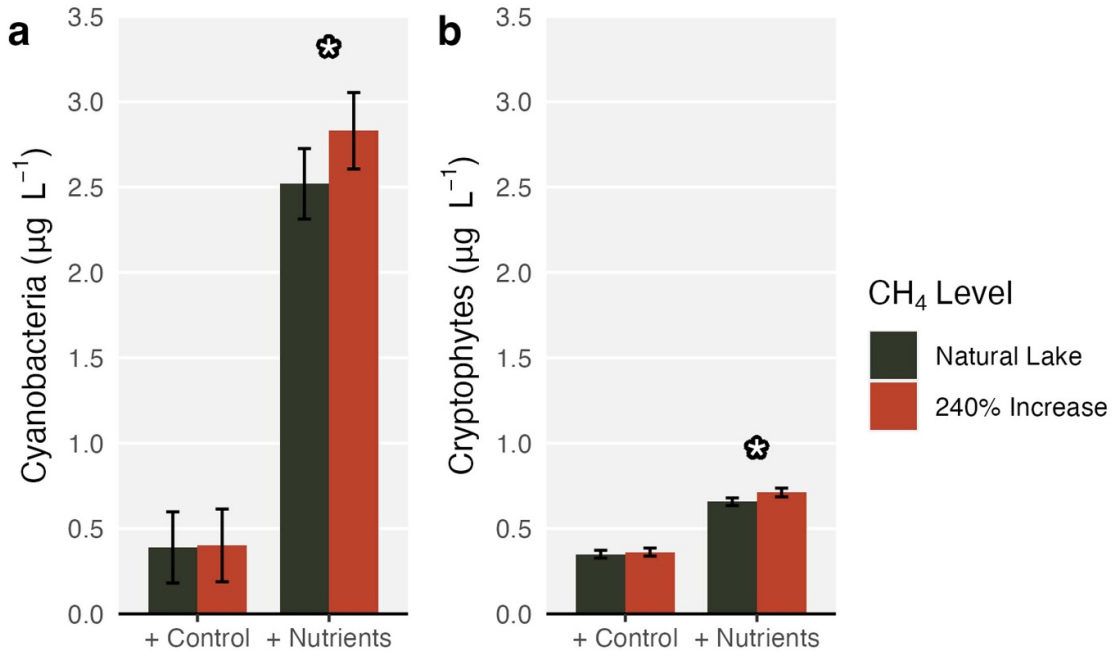


Figure 4. Estimated marginal means of chlorophyll a concentration for (a) cyanobacteria and (b) cryptophytes at two levels of dissolved methane concentration. Standard error is represented for each mean, and asterisks indicate a significant ($P < 0.05$) effect of applied methane treatment for a given nutrient treatment based on linear models.

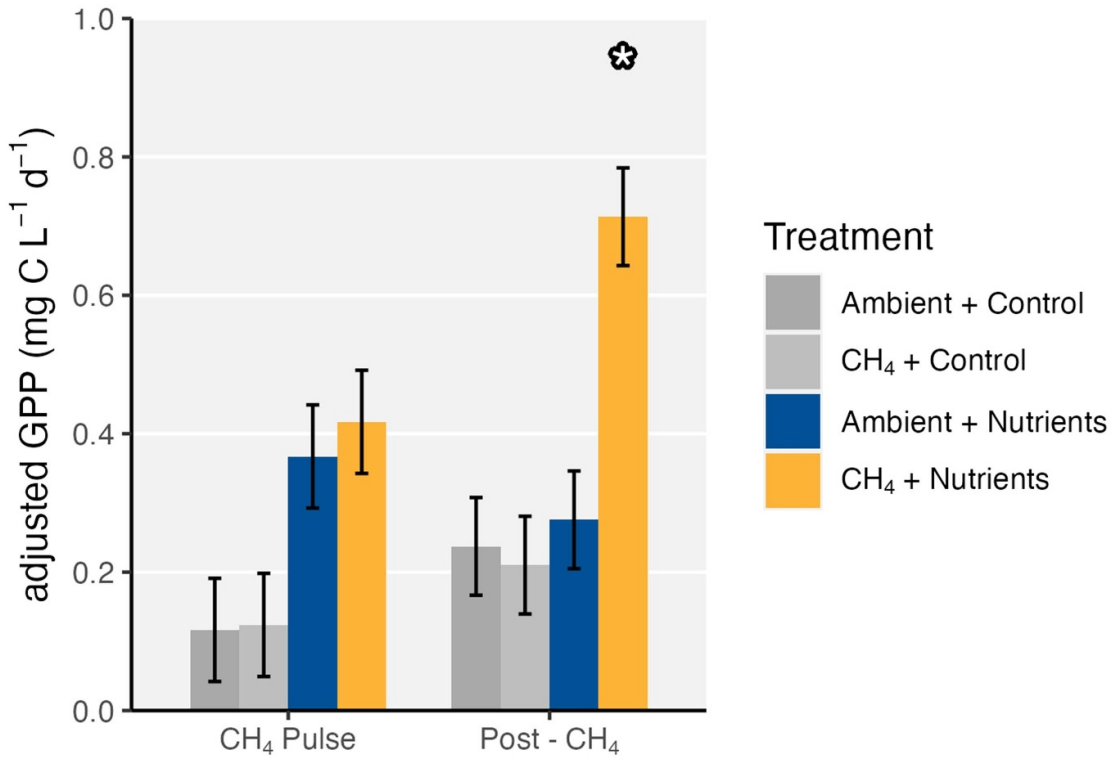


Figure 5. Treatment group means for rates of gross primary production adjusted to a daily mean incident radiation of 500 μmol m^{-2} s^{-1} during the CH_4 pulse period (until day 14) and post-CH_4 (day 15 and onwards). Standard error is represented for each mean, and the asterisk indicates that the GPP in the CH_4 + nutrients treatment group during the post-CH_4 period was significantly different.

the ingestion of MOB, associated (*sensu* Ho *et al* 2014) heterotrophic bacteria or cyanobacteria may have given a slight competitive advantage to Cryptophytes. However, an important caveat is that some cyanobacteria chl a may be misattributed to Cryptophytes with the chemotaxonomic technique used here (Catherine *et al* 2012), in which case this effect may be less or even negligible. It is also important to

note that both of these phytoplankton groups appeared to peak in abundance during the CH_4 pulse and then markedly decline based on chl a concentrations (supporting information figure S6), suggesting that these effects may be short-lived or require sustained high levels of [CH_4].

Regardless of the true underlying mechanism, the relative increase in chl a attributed to phytoplankton groups that are poised to benefit from the conditions that arise amid high CH_4-C levels in eutrophic conditions highlights the importance of nutrient level for these interactions. This partially conflicts with our hypothesis; rather than synergism, these results suggest that high nutrient levels are *required* for elevated [CH_4] to manifest influences on the phytoplankton community.

4.2. Dynamics of ecosystem functioning

The considerable relative increase of GPP observed in the nutrient-enriched mesocosms (>150%) suggests that elevated [CH_4] may have substantial impacts on ecosystem functioning. It is intriguing that adjusted GPP was only significantly greater in the latter half of the experiment once [CH_4] was in decline, and without a corresponding relative increase in phytoplankton chl a. We imagine the mesocosms would have strongly selected for the most effective viral and predator species by the latter half of the experiment, which could have upregulated loss pressures (i.e. lysis, grazing as in figure 1, mechanism 2b) and may have prevented this greater GPP from yielding increased phytoplankton abundance. We find the most plausible explanation is that there was a lagged effect on primary production, which may have eventually disappeared once [CH_4] or derived exudates declined below a critical threshold or the influence of other covariate parameters (e.g. water temperature) waned (supporting information figure S5). Assuming the maximum epilimnetic k as measured in a study of Quebec lakes (0.94 $d^{-1,}$ Thottathil *et al* 2019) and the maximum observed pCH_4 observed here in the mesocosms (5694 μatm), we liberally estimated a CH_4 oxidation rate of 0.090 mg C l^{-1} d^{-1}, which is very likely not realistic based on what was observed in CH_4 incubation data. Regardless, this CH_4 oxidation rate would still only account for ∼20% of the mean estimated increase in GPP if all oxidized CH_4 was converted into CO_2, suggesting that direct supplementation of CO_2 from CH_4 oxidation cannot alone explain the observed increase in GPP.

4.3. Inferring the presence of MOB

Beyond the aforementioned evidence suggesting MOB activity and interactions (figure 1), the notion that MOB were active and thus able to influence the phytoplankton community aligns with further results of this study. The significant net decrease in pCH_4 observed during water sample incubations in mesocosms that were actively being aerated with CH_4-enriched air suggests upregulated CH_4 oxidation rates, thus implying the presence of microbes capable of this process. In fact, inhibition of CH_4 oxidation from light or accumulation of O_2 due to our methodological approach may have reduced the magnitude of this net decrease, as well as obscured other subtle dynamics. Broadly, MOB have much greater cell-specific activity than other heterotrophic bacteria while comprising only a small part of total heterotroph abundance in lakes (Reis *et al* 2022) and thus changes in metabolism may not have manifested proportionate changes in the picoheterotroph cells counts measured here. Further, an experimental study suggested that other microbes may replace MOB cells while they are selectively grazed, thus maintaining total cell counts (Kankaala *et al* 2007). Although not directly measuring the abundance or activity of MOB is certainly a limitation of this study, the absence of plausible alternative explanations for the observed impacts on the phytoplankton community makes interactions based around CH_4-C uptake the most likely cause.

4.4. Other limitations and future work

While the theoretical foundation of this study is based on the pelagic zone (figure 1), periphyton growth may have occurred in the mesocosms, which was not measured and may have had an impact on some of the response variables measured here (e.g. [DOC], GPP). However, as visual evidence of major periphyton growth was not noted during this study and any periphyton present would nonetheless have occupied the same oxic, illuminated conditions this study aimed to represent, we do not consider distinguishing periphytic from planktonic species to be critical in interpreting our results. Indeed, this distinction matters less than a more central limitation: the chemotaxonomic approach used here does not characterize the full breadth of microbial diversity present in the mesocosms, allowing for little inference in terms of the true mechanisms that underpin the effects observed in this study. Generally speaking, not identifying these mechanisms is a critical limitation of this study, and although ultimately deemed out of scope, leaves a clear gap in knowledge that provides opportunity for future study.

Using molecular approaches to characterize the microbial community present (e.g. Zepernick *et al* 2024) could provide insight into the dynamics that gave rise to the observed effects. Leveraging stable

isotopes is an effective way of tracing the uptake and fate of CH_4-C in aquatic ecosystems (Grey 2016) and lends itself to use in this context. In addition, future work could examine the quality of DOC produced under elevated [CH_4] (e.g. biodegradability, metabolomics). Variation in other environmental conditions beyond nutrient level may also influence the importance of CH_4 enrichment. For example, the importance of CH_4-C metabolisms and related microbial interactions may be greater in zones that toggle to and from low O_2 conditions due to factors such as bloom degradation (Barica *et al* 1980), temporary stratification (Andersen *et al* 2017, Davidson *et al* 2024), or the influence of aquatic plants (Andersen *et al* 2017, Aben *et al* 2022). Stated simply, future work could use various methods to understand how and when the uptake of CH_4-C may yield the effects observed here.

4.5. Broader relevance of findings

Overall, these results suggest that microbial interactions involving CH_4-C uptake implicate the phytoplankton community in natural eutrophic settings. It makes sense that some phytoplankton would adapt to capitalize on increases in CH_4-C occurring alongside eutrophication. It is critical to note that the apparent effects of elevated [CH_4] on phytoplankton chl a were modest (∼10% increase in a realistic scenario) and may be better described as a shift in community composition rather than net growth (i.e. did not significantly increase total chl a). In addition, the changes to CH_4 cycling that we observed based on the water sample incubations performed throughout the experiment were minimal (<5% of [CH_4]), and thus were likely not ecologically substantial on their own. Despite this, it is possible that these rather minor effects may have initiated a gradual accumulation of change across the experiment, eventually leading to the more substantial impacts observed on GPP. Further, additionally generated DOC could impact carbon cycling more generally and serve as positive feedback in the global 'browning' of lakes (Solomon *et al* 2015), as the conditions found in more DOC-rich lakes may lead to greater CH_4 production (Williamson *et al* 2015, Jane *et al* 2021). In summation, we conclude that increases in CH_4-C can have biologically relevant effects on carbon transfer and the phytoplankton community in eutrophic settings, which may be an important consideration in understanding how freshwater ecosystems will respond to global change.

Acknowledgments

For their efforts in deploying and maintaining the field experiment, we thank Brian Schatteman, Marcus Lin, and the following student members of the West Island Black Community Association: Karim Ahmad Bélizaire, Jeremy Blackman, Nyla Minnot-Williams, and Michelle Chimdy Onyebuchi. We also thank Misha Ardichvili and Catalina Claus for their help during the pilot phase of the experiment. Dr Egor Katkov and Michelle Gros (McGill University) provided critical assistance in experimental design and methodology. We greatly appreciate the lab of Dr Nagissa Mahmoudi (McGill University) providing sampling materials when they were urgently needed. Dr David Walsh (Concordia University) shared valuable insight into microbial dynamics. Camille Stegen (McGill University) provided critical technical expertise on flow cytometry. We acknowledge the Gault Nature Reserve (McGill University) for providing access to the research site and logistical support and the GRIL-UQAM analytical lab (managed by Katherine Velghe) for providing advice and performing water chemistry analyses.

Data availability statement

The data that support the findings of this study are openly available at the following URL/DOI: https://doi.org/10.5683/SP3/U3U6GY (Gedig and Fussmann 2026).

Supporting Information available at: https://doi.org/10.1088/2752-664X/ae8f50/data1.

Author contributions

Daniel P Gedig 0000-0001-6079-236X
Conceptualization (equal), Investigation (equal), Methodology (equal), Visualization (equal), Writing – original draft (equal)

Gregor F Fussmann
Conceptualization (equal), Funding acquisition (equal), Writing – review & editing (equal)

References

Aben R C H, Velthuis M, Kazanjian G, Frenken T, Peeters E T H M, Van de Waal D B, Hilt S, de Senerpont Domis L N, Lamers L P M and Kosten S 2022 Temperature response of aquatic greenhouse gas emissions differs between dominant plant types *Water Res.* **226** 119251

Andersen M R, Kragh T and Sand-Jensen K 2017 Extreme diel dissolved oxygen and carbon cycles in shallow vegetated lakes *Proc. R. Soc. B* **284** 20171427

Appling A P, Hall R O Jr, Yackulic C B and Arroita M 2018 Overcoming equifinality: leveraging long time series for stream metabolism estimation *J. Geophys. Res. Biogeosci.* **123** 624–45

Badr K, He Q P and Wang J 2022 Identifying interspecies interactions within a model methanotroph-photoautotroph coculture using semi-structured and structured modeling *IFAC-PapersOnLine, 13th IFAC Symp. on Dynamics and Control of Process Systems, Including Biosystems DYCOPS 2022* vol 55 pp 106–11

Barica J, Kling H and Gibson J 1980 Experimental manipulation of algal bloom composition by nitrogen addition *Can. J. Fish. Aquat. Sci.* **37** 1175–83

Bates D, Mächler M, Bolker B and Walker S 2015 Fitting linear mixed-effects models using lme4 *J. Stat. Softw.* **67** 1–48

Beaulieu J J, DelSontro T and Downing J A 2019 Eutrophication will increase methane emissions from lakes and impoundments during the 21st century *Nat. Commun.* **10** 1375

Bizic M 2021 Phytoplankton photosynthesis: an unexplored source of biogenic methane emission from oxic environments *J. Plankton Res.* **43** 822–30

Bogard M J, Del Giorgio P A, Boutet L, Chaves M C G, Prairie Y T, Merante A and Derry A M 2014 Oxic water column methanogenesis as a major component of aquatic CH_4 fluxes *Nat. Commun.* **5** 5350

Byrd R H, Lu P, Nocedal J and Zhu C 1995 A limited memory algorithm for bound constrained optimization *SIAM J. Sci. Comput.* **16** 1190–208

Catherine A, Escoffier N, Belhocine A, Nasri A B, Hamlaoui S, Yéprémian C, Bernard C and Troussellier M 2012 On the use of the FluoroProbe®, a phytoplankton quantification method based on fluorescence excitation spectra for large-scale surveys of lakes and reservoirs *Water Res.* **46** 1771–84

Cerbin S *et al* 2022 Methane-derived carbon as a driver for cyanobacterial growth *Front. Microbiol.* **13** 837198

Clever H L and Young C L (eds) (with Battino, R., & Hayduk, W) 1987 *Methane* vol 27/28 (Pergamons Press)

Cole J J *et al* 2007 Plumbing the global carbon cycle: integrating inland waters into the terrestrial carbon budget *Ecosystems* **10** 172–85

Cole J J and Caraco N F 1998 Atmospheric exchange of carbon dioxide in a low-wind oligotrophic lake measured by the addition of SF6 *Limnol. Oceanogr.* **43** 647–56

Crevecoeur S, Ruiz-González C, Prairie Y T and Del Giorgio P A 2019 Large-scale biogeography and environmental regulation of methanotrophic bacteria across boreal inland waters *Mol. Ecol.* **28** 4181–96

Davidson T A, Søndergaard M, Audet J, Levi E, Esposito C, Bucak T and Nielsen A 2024 Temporary stratification promotes large greenhouse gas emissions in a shallow eutrophic lake *Biogeosciences* **21** 93–107

Del Giorgio P A, Bird D F, Prairie Y T and Planas D 1996 Flow cytometric determination of bacterial abundance in lake plankton with the green nucleic acid stain SYTO 13 *Limnol. Oceanogr.* **41** 783–9

Devlin S P, Saarenheimo J, Syväranta J and Jones R I 2015 Top consumer abundance influences lake methane efflux *Nat. Commun.* **6** 8787

Garcia H E and Gordon L I 1992 Oxygen solubility in seawater: better fitting equations *Limnol. Oceanogr.* **37** 1307–12

Gedig D P and Fussmann G F 2026 Experimental Data from Methane-Enriched Freshwater Mesocosms at Gault Nature Reserve [Quebec, Canada, 2024] *Borealis* (https://doi.org/10.5683/SP3/U3U6GY)

Glibert P M 2024b The phycosphere-living and dying in close quarters *Phytoplankton Whispering: An Introduction to the Physiology and Ecology of Microalgae* (Springer) pp 483–501

Glibert P M 2024a Mixotrophy: microbial Multitasking *Phytoplankton Whispering: An Introduction to the Physiology and Ecology of Microalgae* ed P M Glibert (Springer) pp 329–58

Grey J 2016 The incredible lightness of being methane-fuelled: stable isotopes reveal alternative energy pathways in aquatic ecosystems and beyond *Front. Ecol. Evol.* **4** 8

Hall R O Jr, Yackulic C B, Kennedy T A, Yard M D, Rosi-Marshall E J, Voichick N and Behn K E 2015 Turbidity, light, temperature, and hydropeaking control primary productivity in the Colorado River, Grand Canyon *Limnol. Oceanogr.* **60** 512–26

Ho A, Angel R, Veraart A J, Daebeler A, Jia Z, Kim S Y, Kerckhof F-M, Boon N and Bodelier P L E 2016 Biotic interactions in microbial communities as modulators of biogeochemical processes: methanotrophy as a model system *Front. Microbiol.* **7** 1285

Ho A, de Roy K, Thas O, De Neve J, Hoefman S, Vandamme P, Heylen K and Boon N 2014 The more, the merrier: heterotroph richness stimulates methanotrophic activity *ISME J.* **8** 1945–8

Holgerson M A and Raymond P A 2016 Large contribution to inland water CO_2 and CH_4 emissions from very small ponds *Nat. Geosci.* **9** 222–6

Jane S F *et al* 2021 Widespread deoxygenation of temperate lakes *Nature* **594** 66–70

Jones R I and Grey J 2011 Biogenic methane in freshwater food webs *Freshw. Biol.* **56** 213–29

Kankaala P, Eller G and Jones R I 2007 Could bacterivorous zooplankton affect lake pelagic methanotrophic activity? *Fundam. Appl. Limnol.* **169** 203–9

Katkov E and Fussmann G F 2023 The effect of increasing temperature and pCO_2 on experimental pelagic freshwater communities *Limnol. Oceanogr.* **68** S202–S16

Katkov E, Low-Décarie É and Fussmann G F 2020 Intra-annual variation of phytoplankton community responses to factorial N, P, and CO_2 enrichment in a temperate mesotrophic lake *Freshw. Biol.* **65** 960–70

Koschorreck M, Prairie Y T, Kim J and Marcé R 2021 Technical note: CO_2 is not like CH_4—limits of and corrections to the headspace method to analyse pCO_2 in fresh water *Biogeosciences* **18** 1619–27

Kuznetsova A, Brockhoff P B and Christensen R H B 2017 lmerTest package: tests in linear mixed effects models *J. Stat. Softw.* **82** 1–26

Le Noac'h P, Cremella B, Kim J, Soria-Píriz S, Del Giorgio P A, Pollard A I, Huot Y and Beisner B E 2024 Nutrient availability is the main driver of nanophytoplankton phago-mixotrophy in North American lake surface waters *J. Plankton Res.* **46** 9–24

Lenth R 2024 *emmeans: Estimated Marginal Means, aka Least-Squares Means (Version 1.10.5)* (Computer software) (available at: https://CRAN.R-project.org/package=emmeans)
Li C *et al* 2021 Global co-occurrence of methanogenic archaea and methanotrophic bacteria in Microcystis aggregates *Environ. Microbiol.* **23** 6503–19
Li X, He M, Shi Z and Xu J 2023 Nutritional status regulates bacteria-virus interactions in the Northern South China Sea *J. Geophys. Res. Biogeosci.* **128** e2023JG007469
Li X, Lu Y, Li N, Wang Y, Yu R, Zhu G and Zeng R J 2022 Mixotrophic cultivation of microalgae using biogas as the substrate *Environ. Sci. Technol.* **56** 3669–77
Model M A 2018 Methods for cell volume measurement *Cytometry A* **93** 281–96
Murase J and Sugimoto A 2005 Inhibitory effect of light on methane oxidation in the pelagic water column of a mesotrophic lake (Lake Biwa, Japan) *Limnol. Oceanogr.* **50** 1339–43
Nijman T P A, Davidson T A, Weideveld S T J, Audet J, Esposito C, Levi E E, Ho A, Lamers L P M, Jeppesen E and Veraart A J 2021 Warming and eutrophication interactively drive changes in the methane-oxidizing community of shallow lakes *ISME Commun.* **1** 32
Odum H T 1956 Primary production in flowing waters *Limnol. Oceanogr.* **1** 102–17
Olson R J, Zettler E R and Anderson O K 1989 Discrimination of eukaryotic phytoplankton cell types from light scatter and autofluorescence properties measured by flow cytometry *Cytometry* **10** 636–43
Oswald K *et al* 2017 Crenothrix are major methane consumers in stratified lakes *ISME J.* **11** 2124–40
Pascault N, Rué O, Loux V, Pédron J, Martin V, Tambosco J, Bernard C, Humbert J-F and Leloup J 2021 Insights into the cyanosphere: capturing the respective metabolisms of cyanobacteria and chemotrophic bacteria in natural conditions? *Environ. Microbiol. Rep.* **13** 364–74
Patton C J and Kryskalla J R 2003 Methods of analysis by the U.S. Geological Survey National Water Quality Laboratory-Evaluation of alkaline persulfate digestion as an alternative to Kjeldahl digestion for determination of total and dissolved nitrogen and phosphorus in water *Water-Resources Investigations Report* pp 2003–4174 (https://doi.org/10.3133/wri034174)
Perez-Coronel E and Beman J M 2022 Multiple sources of aerobic methane production in aquatic ecosystems include bacterial photosynthesis *Nat. Commun.* **13** 6454
Pernthaler J 2017 Competition and niche separation of pelagic bacteria in freshwater habitats *Environ. Microbiol.* **19** 2133–50
Posit Team 2023 *RStudio: Integrated Development Environment for R [Computer software]* (Posit Software, PBC) (available at: www.posit.co/)
R Core Team 2024 *R: A Language and Environment for Statistical Computing* (Version 4.4.2) [Computer software] (R Foundation for Statistical Computing) (available at: www.R-project.org/)
Raymond P A, Zappa C J, Butman D, Bott T L, Potter J, Mulholland P, Laursen A E, McDowell W H and Newbold D 2012 Scaling the gas transfer velocity and hydraulic geometry in streams and small rivers *Limnol. Oceanogr. Fluids Environ.* **2** 41–53
Regnier P, Resplandy L, Najjar R G and Ciais P 2022 The land-to-ocean loops of the global carbon cycle *Nature* **603** 401–10
Reis P C J, Thottathil S D and Prairie Y T 2022 The role of methanotrophy in the microbial carbon metabolism of temperate lakes *Nat. Commun.* **13** 43
Reis P C J, Tsuji J M, Weiblen C, Schiff S L, Scott M, Stein L Y and Neufeld J D 2024 Enigmatic persistence of aerobic methanotrophs in oxygen-limiting freshwater habitats *ISME J.* **18** wrae041
Rissanen A J, Saarenheimo J, Tiirola M, Peura S, Aalto S L, Karvinen A and Nykänen H 2018 Gammaproteobacterial methanotrophs dominate methanotrophy in aerobic and anaerobic layers of boreal lake waters *Aquat. Microb. Ecol.* **81** 257–76
Rooney N and Kalff J 2003 Interactions among epilimnetic phosphorus, phytoplankton biomass and bacterioplankton metabolism in lakes of varying submerged macrophyte cover *Hydrobiologia* **501** 75–81
Salzman G C 1999 Light scatter: detection and usage *Curr. Protoc. Cytom.* **9** 1.13.1–8
Saunois M *et al* 2020 The global methane budget 2000–2017 *Earth Syst. Sci. Data* **12** 1561–623
Schilder J, van Hardenbroek M, Bodelier P, Kirilova E P, Leuenberger M, Lotter A F and Heiri O 2017 Trophic state changes can affect the importance of methane-derived carbon in aquatic food webs *Proc. R. Soc. B* **284** 20170278
Sieburth J M, Smetacek V and Lenz J 1978 Pelagic ecosystem structure: heterotrophic compartments of the plankton and their relationship to plankton size fractions 1 *Limnol. Oceanogr.* **23** 1256–63
Solomon C T *et al* 2015 Ecosystem consequences of changing inputs of terrestrial dissolved organic matter to lakes: current knowledge and future challenges *Ecosystems* **18** 376–89
Staehr P A, Bade D, Van de Bogert M C, Koch G R, Williamson C, Hanson P, Cole J J and Kratz T 2010 Lake metabolism and the diel oxygen technique: state of the science *Limnol. Oceanogr.: Methods* **8** 628–44
Takahashi T 2019 Routine management of microalgae using autofluorescence from chlorophyll *Molecules* **24** 4441
Thimijan R W and Heins R D 1983 Photometric, radiometric, and quantum light units of measure: a review of procedures for interconversion *HortScience* **18** 818–22
Thottathil S D, Reis P C J and Prairie Y T 2019 Methane oxidation kinetics in northern freshwater lakes *Biogeochemistry* **143** 105–16
Thottathil S D, Reis P C J and Prairie Y T 2022 Magnitude and drivers of oxic methane production in small temperate lakes *Environ. Sci. Technol.* **56** 11041–50
Tranvik L J, Porter K G and Sieburth J M 1989 Occurrence of bacterivory in Cryptomonas, a common freshwater phytoplankter *Oecologia* **78** 473–6
Weiss R F 1974 Carbon dioxide in water and seawater: the solubility of a non-ideal gas *Mar. Chem.* **2** 203–15
Wetzel R G and Likens G E 2000 Inorganic nutrients: nitrogen, phosphorus, and other nutrients *Limnological Analyses* ed R G Wetzel and G E Likens (Springer) pp 85–111
Wickham H 2016 *Ggplot2: Elegant Graphics for Data Analysis* (Springer) (https://doi.org/10.1007/978-3-319-24277-4)
Williamson C E, Overholt E P, Pilla R M, Leach T H, Brentrup J A, Knoll L B, Mette E M and Moeller R E 2015 Ecological consequences of long-term browning in lakes *Sci. Rep.* **5** 18666
Winslow L A, Zwart J A, Batt R D, Dugan H A, Woolway R I, Corman J R, Hanson P C and Read J S 2016 LakeMetabolizer: an R package for estimating lake metabolism from free-water oxygen using diverse statistical models *Inland Waters* **6** 622–36
Zepernick B N *et al* 2024 Molecular investigation of harmful cyanobacteria reveals hidden risks and niche partitioning in Kenyan Lakes *Harmful Algae* **140** 102757